Pharmacology, Biochemistry and Behavior 187 (2019) 172794

Contents lists available at ScienceDirect

Pharmacology, Biochemistry and Behavior

journal homepage: www.elsevier.com/locate/pharmbiochembeh

TAK-925, an orexin 2 receptor-selective agonist, shows robust wake-promoting effects in mice

Hiroshi Yukitake, Tatsuhiko Fujimoto, Takashi Ishikawa, Atsushi Suzuki, Yuji Shimizu, Kentaro Rikimaru, Mitsuhiro Ito, Motohisa Suzuki, Haruhide Kimura*

Neuroscience Drug Discovery Unit, Research, Takeda Pharmaceutical Company Limited, Fujisawa, Japan

ARTICLE INFO

Keywords:
Orexin
Orexin 2 receptor
Orexin 2 receptor agonist
TAK-925
Hypersomnia
Narcolepsy

ABSTRACT

Orexin-producing neurons in the lateral hypothalamus are a critical regulator of sleep/wake states, and their loss is associated with narcolepsy type 1 (NT1). Orexin peptides act on two G protein-coupled receptors: orexin 1 receptor (OX1R) and orexin 2 receptor (OX2R). OX2R knockout (KO) mice, but not OX1R KO mice, showed clear narcolepsy-like phenotypes, including fragmented sleep-wake cycles. Moreover, OX2R-selective antagonists have been shown to induce sleepiness in mice, and activation of OX2R has been reported to increase wakefulness. In this study, we characterized *in vitro* and *in vivo* profiles of a novel, highly selective OX2R agonist, TAK-925 [methyl (2*R*,3*S*)-3-[(methylsulfonyl)amino]-2-{[(*cis*-4-phenylcyclohexyl)oxy]methyl}piperidine-1-carboxylate]. TAK-925 activated human recombinant OX2R with 50% effective concentration value of 5.5 nM, and showed > 5,000-fold selectivity over OX1R in calcium mobilization assays. TAK-925 induced OX2R-downstream signals similar to those displayed by orexin peptides in Chinese hamster ovary cells stably expressing human OX2R. In an electrophysiological study, TAK-925 activated physiological OX2R on histaminergic neurons in the mouse tuberomammillary nucleus (TMN). Subcutaneous (SC) administration of TAK-925 also modulated neuronal activity in various brain regions, including TMN, as measured by an immunohistochemical analysis using an anti-c-fos antibody. TAK-925 (SC) increased wakefulness in wild-type mice, but not in OX2R KO mice, during their sleep phase, demonstrating that a highly selective OX2R agonist can increase wakefulness in mice *via* OX2R activation. TAK-925 may have therapeutic potential to reduce hypersomnia in multiple disorders including NT1.

1. Introduction

The orexin (hypocretin) system plays an important role in the regulation of anxiety/emotion, reward/drug addiction, feeding/energy homeostasis, and sleep/wakefulness (Tsujino and Sakurai, 2009). Orexin-producing neurons (orexin neurons) in the lateral hypothalamus project to multiple networks of monoaminergic, cholinergic, and histaminergic neurons throughout the brain and brain stem excluding the cerebellum (Marcus et al., 2001; Sakurai, 2007). The orexin peptides, orexin A peptide (OX-A) and orexin B peptide (OX-B), are produced by proteolytic cleavage of a single precursor polypeptide, prepro-orexin, in orexin neurons (de Lecea et al., 1998; Sakurai et al., 1998). There are two postsynaptic G protein-coupled receptors (GPCRs) for orexin peptides, orexin 1 receptor (OX1R) and orexin 2 receptor (OX2R) (Sakurai et al., 1998). OX1R has one order of magnitude higher binding affinity for OX-A over OX-B, whereas OX2R binds to both peptides with similar affinities (Sakurai et al., 1998). The two orexin receptors exhibit basically complementary expression patterns, supporting distinct

Abbreviations: ACSF, artificial cerebrospinal fluid; BBB, blood-brain barrier; BSA, bovine serum albumin; CHO, Chinese hamster ovary; CREB, cAMP response element binding protein; CSF, cerebrospinal fluid; DMSO, dimethyl sulfoxide; EC_{50}, 50% effective concentration; EDS, excessive daytime sleepiness; EDTA, ethylenediaminetetraacetic acid; EEG, electroencephalogram; EMG, electromyogram; ERK, extracellular signal-regulated kinase; FBS, fetal bovine serum; GPCR, G protein-coupled receptor; h, human; HBSS, Hank's balanced salt solution; HDR, homology-directed repair; HEPES, 2-[4-(2-Hydroxyethyl)-1-piperazinyl]ethanesulfonic acid; HTRF, homogenous time-resolved fluorescence resonance energy transfer; IC_{50}, 50% inhibitory concentration; ICV, intracerebroventricular; IP1, inositol monophosphate; KO, knockout; LC, locus ceruleus; NREM, non-rapid eye movement; NT1, narcolepsy type 1; OX-A, orexin A peptide; OX-B, orexin B peptide; OX1R, orexin 1 receptor; OX2R, orexin 2 receptor; PPN, pedunculopontine nucleus; qPCR, quantitative polymerase chain reaction; REM, rapid eye movement; ROI, region of interest; SC, subcutaneous or subcutaneously; SCH, suprachiasmatic nucleus; ssODN, single-stranded oligodeoxynucleotide; TMN, tuberomammillary nucleus; TTX, tetrodotoxin; VLP, virus-like particle; WT, wild-type; ZT, zeitgeber time

* Corresponding author at: Neuroscience Drug Discovery Unit, Research, Takeda Pharmaceutical Company Limited, 26-1, Muraoka-Higashi 2-chome, Fujisawa, Kanagawa 251-8555, Japan.

E-mail address: haruhide.kimura@takeda.com (H. Kimura).

https://doi.org/10.1016/j.pbb.2019.172794
Received 11 September 2019; Received in revised form 1 October 2019; Accepted 1 October 2019
Available online 22 October 2019

physiological roles.

Several studies have demonstrated that loss of orexin neurons in the lateral hypothalamus and the resulting orexin deficiency in the brain are associated with narcolepsy type 1 (NT1) (Nishino et al., 2000; Peyron et al., 2000; Thannickal et al., 2000). For example, postmortem studies measuring expression levels of prepro-orexin mRNA or orexin-peptides revealed an 85%–100% reduction of orexin neurons in patients with NT1 (Peyron et al., 2000; Thannickal et al., 2000). OX-A level in cerebrospinal fluid (CSF) in patients with NT1 is 110 pg/mL or less, or less than one-third of the mean value obtained in normal individuals (Sateia, 2014; Golden and Lipford, 2018); normal CSF OX-A levels are above 200 pg/mL regardless of gender, age and time of the CSF collections (Nishino and Kanbayashi, 2005). Moreover, narcolepsy-like symptoms, such as sleep/wake fragmentation, direct transitions from wakefulness to rapid eye movement (REM) sleep, and cataplexy-like episodes occurred in both prepro-orexin-knockout mice (KO), and in orexin/ataxin-3 mice whose orexin neurons were degraded by induction of the neurotoxic polyglutamine repeat of the ataxin-3 protein (Hara et al., 2001; Mieda et al., 2004).

Importantly, OX2R KO mice exhibited both a fragmentation of sleep/wake states and cataplexy-like episodes, while OX1R KO mice had no overt behavioral abnormalities and exhibited only mild fragmentation of sleep/wake cycles (Tsujino and Sakurai, 2009). Dogs with null mutations in the *Hcrtr2* genes showed remarkable narcolepsy-like phenotypes, such as robust fragmentation of wakefulness and clear cataplexy-like episodes (Lin et al., 1999). Moreover, OX2R selective antagonists, such as MIN-202 and MK-1064, can induce sleepiness (Jacobson et al., 2017). Thus, OX2R appears to play a pivotal role in the pathophysiology of NT1 compared with OX1R.

Currently available medications for NT1, including psychostimulants (eg, modafinil and methylphenidate for excessive daytime sleepiness [EDS]), antidepressants (including clomipramine and venlafaxine for cataplexy), and sedatives (sodium oxybate for both EDS and cataplexy) are all symptomatic treatments with limited efficacy and adverse effects (Inoue et al., 2013; Thorpy, 2015; Barateau et al., 2016). Because NT1 results from loss of orexins, replacement therapies with orexin peptides or orexin receptor agonists are considered to be promising therapeutic options for NT1. In fact, narcolepsy-like symptoms in orexin/ataxin-3 mice were ameliorated by intracerebroventricular (ICV) administration of orexin peptides, indicating that orexin receptors and their downstream neural pathways remain functionally intact even after experiencing long-term orexin deficiency in mice (Mieda et al., 2004). Orexin peptides, however, do not penetrate the blood-brain barrier (BBB), and are not suitable for clinical use as drugs (Fujiki et al., 2003). In addition, activation of OX1R in the ventral tegmental area by orexin peptides may lead to addictive behaviors *via* activation of the dopaminergic reward system (Nakamura et al., 2000; Xu et al., 2013). Overall, OX2R-selective agonists would be preferred over OX1R/OX2R dual agonists as a novel therapy for NT1 based on theoretical potent efficacy and lower risks of abuse liability (Willie et al., 2003; Tsujino and Sakurai, 2009). Recently, investigators at University of Tsukuba reported the discovery of a novel OX2R agonist, YNT-185, which increased wakefulness in wild-type (WT) mice during their sleep phase and suppressed cataplexy-like episodes in orexin KO mice and orexin/ataxin-3 mice during their active phase (Nagahara et al., 2015; Irukayama-Tomobe et al., 2017).

Using high-throughput screening followed by lead optimization of active compounds, we discovered a novel, small-molecule OX2R-selective agonist, TAK-925 [methyl (2*R*,3*S*)-3-[(methylsulfonyl)amino]-2-{[(*cis*-4-phenylcyclohexyl)oxy]methyl}piperidine-1-carboxylate]. In this study, we have characterized the *in vitro* and *in vivo* profiles of TAK-925. Our data show that TAK-925 has the potential to be developed as a new therapy for hypersomnia disorders including NT1.

2. Materials and methods

2.1. Animals

Three- to 4-week-old male C57BL/6 mice obtained from CLEA Japan Inc. (Tokyo, Japan) were used for slice electrophysiology studies. Orexin/ataxin-3 mice with a C57BL/6J genetic background were introduced from University of Tsukuba under a material transfer agreement. Orexin/ataxin-3 mice were bred in our laboratory, and male orexin/ataxin-3 mice aged 35 weeks were used for c-fos staining. OX2R KO mice were generated in our laboratory. Twelve- to 13-week-old male C57BL/6J mice and OX2R KO mice were used for electroencephalogram/electromyogram (EEG/EMG) studies. All mice were housed under laboratory conditions (12 h light/dark cycles) with food (CE-2, CLEA Japan Inc.) and water available *ad libitum*. The care and use of the animals and the experimental protocols in this study conducted in Takeda were approved by the Institutional Animal Care and Use Committee of Takeda Pharmaceutical Company Limited.

2.2. Chemicals and radiolabeled ligand

TAK-925 and compound 1 m [(3*R*,5*S*)-4-(4-Chlorobenzoyl)-7-(difluoromethoxy)-3,5-dimethyl-2,3,4,5-tetrahydro-1,4-benzoxazepine] were synthesized by Takeda Pharmaceutical Company Limited. Compound 1 m was reported to be a potent and selective OX2R antagonist (50% inhibitory concentration (IC_{50}) = 27 nM with 100-fold selectivity against OX1R) (Fujimoto et al., 2011). [^{3}H]T-516 (777 GBq/mL) was synthesized by BioBridge K.K. (Tokyo, Japan).

2.3. Antibodies

Antibodies and their sources were as follows: anti-c-Fos (9F6) rabbit monoclonal antibody from Cell Signaling Technology (Cat#2250; RRID: AB_2247211, MA, USA); biotin-SP-conjugated AffiniPure donkey anti-rabbit IgG (H + L) from Jackson Immuno Research (Cat.# 711-065-152; RRID: AB_2340593, PA, USA).

2.4. Cell lines and culture

Chinese hamster ovary-K1 (CHO-K1) cells (CCL-61, ATCC) stably expressing human (h) OX1R or OX2R (hOX1R/CHO-K1 cells or hOX2R/CHO-K1 cells) were established as follows: The hOX1R or hOX2R gene was subcloned into pcDNA3.1(+) Zeo mammalian expression vectors (Cat.# X86020, Thermo Fisher Scientific Inc., MA, USA). OX1R or OX2R expression vectors (pcDNA3.1(+)-hOX1R and pcDNA3.1(+)-hOX2R) were introduced into CHO-K1 cells using the Gene Pulser II Electroporation System (Cat.# 1652660 J1, Bio-Rad Laboratories, Inc., CA, USA) and then G-418 Sulfate (Thermo Fisher Scientific Inc.) resistant clones were selected as hOX1R/CHO-K1 or hOX2R/CHO-K1 cells. hOX1R/CHO-K1 cells or hOX2R/CHO-K1 cells were used for a calcium mobilization assay.

CHO cells stably expressing ProLink-tagged hOX2R and β-arrestin2 coupled to an inactive N-terminal β-galactosidase deletion mutant termed enzyme acceptor (β-arrestin2-β-gal-EA fusion) (hOX2R/CHO-EA cells) were established as follows: The hOX2R gene was subcloned into the pCMV-ProLink vector (Cat.# 93-0167, DiscoveRx, CA, USA). pCMV-ProLink-hOX2R vector was introduced into CHO-K1-expressing β-arrestin EA cells (Cat.# 93-0521, DiscoveRx), and then G-418 sulfate-resistant colonies were selected. These cell lines were cultured in growth medium (Modified Eagle Medium alpha) with 10% fetal bovine serum (FBS), 500 μg/mL geneticin (Thermo Fisher Scientific Inc.), and 100 U/mL penicillin-streptomycin (Thermo Fisher Scientific Inc.) at 37 °C in the presence of 5% CO_2. hOX2R/CHO-EA cells were used for the inositol monophosphate (IP1) assay, β-arrestin recruitment assay, and evaluations of phosphorylation of extracellular signal-regulated kinase 1/2 (ERK1/2) and cAMP response element binding protein

(CREB).

Expi293F cells were purchased from Thermo Fisher Scientific Inc. (Cat.# A14527). This cell line was cultured in Expi293™ Expression Medium (Cat.# A1435101, Thermo Fisher Scientific Inc.). Expi293F cells were used for the [^{3}H]T-516 binding assay.

2.5. Generation of OX2R KO mice

Microinjection into mouse embryos was conducted as follows: Cas9 mRNA (L-6125, TriLink BioTechnologies, CA, USA), two single-guide RNAs (sgRNAs) (sgRNA1: GCCCGAAGUUGCCGGGC GCAguuuuagagcuagaaauagcaaguuaaaauaaggcuaguccguuaucaacuu-gaaaaaguggcaccgagucggugcuuuu, sgRNA2: GGGUUAAGAAGUGGUAA CGAguuuuagagcuagaaauagcaaguuaaaauaaggcuaguccguuaucaacuu-gaaaaaguggcaccgagucggugcuuuu) (FASMAC, Kanagawa, Japan) used for *Hcrtr2* exon 1 deletion, and single-stranded oligodeoxynucleotides (ssODNs) (ssODN for homology-directed repair (HDR) donor: gcttctcctggtgcaaatcccctgcaaaga-cactgaagcagcagcccgaagttgccgggccgaaggggcagagtggaggcaaaggcagaca-gaggagcgcgctccatcgcaaaagcagaa) (FASMAC) used for HDR donors were diluted and mixed in 0.1 × TE buffer (10 mM Tris-HCl, 1 mM ethylenediaminetetraacetic acid (EDTA), pH 8.0) to a working concentration of 100 ng/μL, 50 ng/μL, and 50 ng/μL, respectively. The mixture was then injected into the cytoplasm of C57BL/6J zygotes using a micromanipulator and a microinjector. After incubation at 37 °C for 24 h, two-cell-stage embryos were transferred into the oviducts of pseudopregnant ICR females (CLEA Japan Inc.).

Genotyping to screen for homogeneous KO mice was then carried out as follows: Genomic DNA was extracted from the ear of each offspring using a DNeasy Kit or a Puregene Kit (QIAGEN, Hilden, Germany) in accordance with the manufacturer's protocol. For the screening of OX2R KO mice, the copy number of the *Hcrtr2* gene was analyzed by quantitative polymerase chain reaction (qPCR) using the genomic DNA as a template. qPCR was performed using TaqMan Fast Universal PCR Master Mix (Life Technologies, CA, USA) and a TaqMan MGB probe designed to cover *Hcrtr2* exon 1. To confirm the deletion of the *Hcrtr2* exon 1 region, PCR was performed using primers flanking the target region of the *Hcrtr2* gene (5′-ttccagcttcatctctctgtccctc-3′, 5′-aaactgataacaaccacttgcgcgg-3′). The PCR product sizes were 1,268 bp for WT allele and 444 bp for KO allele.

2.6. Drug preparations

For the binding assay, calcium mobilization assay, and β-arrestin assay, TAK-925, OX-A (Cat.# 4346, Peptide Institute Inc., Osaka, Japan) and OX-B (Cat.# 4348, Peptide Institute Inc.) in dimethyl sulfoxide (DMSO) were diluted in assay buffer (Hank's balanced salt solution (HBSS) (Life Technologies)) with 20 mM 2-[4-(2-Hydroxyethyl)-1-piperazinyl]ethanesulfonic acid (HEPES) (Life Technologies), pH 7.4, and 0.1% fatty acid-free bovine serum albumin (BSA, Fujifilm Wako Pure Chemical Co., Osaka, Japan). The final percentage of DMSO was 0.3%, 0.11%, and 0.3% for the binding assay, calcium mobilization assay, and β-arrestin assay, respectively. For the IP1 assay, TAK-925, OX-A and OX-B dissolved in DMSO were diluted in IP1 stimulation buffer (Cisbio Bioassays, Codolet, France) containing 0.1% fatty acid-free BSA. The final percentage of DMSO was 0.3%. For the slice electrophysiology study, TAK-925 and compound 1 m dissolved in DMSO were diluted in artificial cerebrospinal fluid (ACSF) solution (124 mM NaCl, 5 mM KCl, 1.2 mM NaH_2PO_4, 1.5 mM $MgCl_2$, 2.5 mM $CaCl_2$, 10 mM glucose, and 24 mM $NaHCO_3$), and were applied by bath perfusion. The final percentage of DMSO was 0.1%. [Ala^{11}, D-Leu^{15}]-OX-B (Cat.# 2142, Tocris Bioscience, Bristol, UK) in distilled water was diluted in ACSF solution, and was applied by bath perfusion. For *in vivo* evaluation, TAK-925 suspended in 0.5% methylcellulose saline was administered subcutaneously (SC) to mice in a volume of 10 mL/kg of body weight. [Ala^{11}, D-Leu^{15}]-OX-B dissolved in saline was administered ICV to mice in 2.0 μL.

2.7. In vitro study

2.7.1. [^{3}H]T-516 Binding assay

The binding assay was performed using a tritium-labeled OX2R agonist, [^{3}H]T-516, which possesses a chemical scaffold similar to that of TAK-925, and membrane fractions from cells expressing hOX2R-containing virus-like-particles (VLPs). To produce the latter, the hOX2R gene was subcloned into pcDNA3.1 expression vector (Cat.# V79020, Thermo Fisher Scientific Inc.). HIV-1 Gag gene (AAF43628) was subcloned into pcDNA3.3 expression vector (Cat.# K830001, Thermo Fisher Scientific Inc.). Expi293F cells were cultured in Expi293™ Expression Medium (Thermo Fisher Scientific Inc.) and then co-transfected with pcDNA3.1/hOX2R and pcDNA3.3/Gag vector (ratio 2:1) using the ExpiFectamine™ 293 Transfection Kit (Cat.# A14524, Thermo Fisher Scientific Inc.) in accordance with the manufacturer's instructions. After a 72-h incubation, the VLPs containing the OX2R protein were harvested by centrifugation into a pellet (54000 × *g* for 1 h at 4 °C). The VLP pellet was collected and re-suspended in 20 mM Tris-HCl, pH 7.5, 5 mM EDTA, and cOmplete (Cat.# 11873580001 Sigma-Aldrich, Tokyo, Japan) buffer, and the suspension was homogenized using a Dounce Tissue Grinder (PerkinElmer Inc., MA, USA). This homogenate was defined as the hOX2R-expressing membrane preparation. The membrane preparation (10 μg of protein/well) was incubated with various concentrations of TAK-925 and 50 nM [^{3}H]T-516 for 4 h at room temperature in assay buffer (20 mM HEPES, pH 7.4, 100 mM NaCl, 10 mM $MgCl_2$, and 0.1% BSA). The reaction was terminated by rapid filtration through polyethyleneimine-coated GF/C filter plates (PerkinElmer Inc.) using a cell harvester (PerkinElmer Inc.). The filter plates were washed 4 times with 50 mM Tris-HCl, pH 7.5, and dried at 42 °C. Microscint 0 (Cat.# 6013611, PerkinElmer Inc.) was added to each well, and the radioactivity was measured using a TopCount Microplate Scintillation Counter (PerkinElmer Inc.). Nonspecific binding was defined as labeling in the presence of 100 μM unlabeled T-516. The responses to 100 μM unlabeled T-516 and 0.3% DMSO were used to represent the 0% and 100% responses, respectively.

2.7.2. Calcium mobilization assay

hOX1R/CHO-K1 cells and hOX2R/CHO-K1 cells suspended in Ham's F-12 medium (Fujifilm Wako Pure Chemical Co.) supplemented with 100 U/mL penicillin-streptomycin and 10% FBS were plated in black-walled clear-bottomed 384-well plates (Corning, NY, USA) at 10000 cells/well and in black-walled clear-bottomed 96-well plates (Corning) at 45000 cells/well, respectively. The plated cells were grown overnight at 37 °C in the presence of 5% CO_2. The following day, the medium was removed, and the cells were incubated with assay buffer (HBSS with 20 mM HEPES, pH 7.4, and 0.1% fatty acid free BSA) containing 2.5 μg/mL Fluo-4 AM (Cat.# F312, Dojindo Laboratories, Kumamoto, Japan), 1.25 mM probenecid (Dojindo Laboratories), and 0.08% Pluronic F127 (Dojindo Laboratories) for 30 min at 37 °C in the presence of 5% CO_2. After incubation, the cells were stimulated with test compounds in the assay buffer. Calcium mobilization was measured using an FDSS/μCELL (Hamamatsu Photonics K.K., Shizuoka, Japan). The responses to 0.11% DMSO and 100 nM OX-A were used to represent the 0% and 100% responses, respectively.

2.7.3. IP1 assay

Intracellular accumulation of IP1 was measured using an IP-One Homogeneous Time-Resolved Fluorescence Resonance Energy Transfer (HTRF) assay kit (Cat.# 62IPAPEB, Cisbio Bioassays). hOX2R/CHO-EA cells (5000 cells/well) were stimulated with test compounds for 4 h at 37 °C in IP1 stimulation buffer containing 0.1% BSA. The medium was then removed, and IP1-d2 conjugate and anti-IP1 cryptate Tb in lysis buffer were added to each well in accordance with the manufacturer's instructions. The plates were incubated for at least 1 h at room

temperature and read using an EnVision plate reader (PerkinElmer Inc.). The responses to 0.3% DMSO and 1 μM OX-A were used to represent the 0% and 100% responses, respectively.

2.7.4. β-Arrestin recruitment assay

hOX2R/CHO-EA cells were plated in white 384-well plates (5,000 cells/well) in Ham's F-12 medium supplemented with 100 U/mL penicillin-streptomycin and 10% FBS. The plated cells were grown overnight at 37 °C in the presence of 5% CO_2. The following day, the medium was changed and the cells were stimulated with test compounds for 2 h at 37 °C. The binding of β-arrestin to the receptor was assessed using a PathHunter assay kit (DiscoveRx), in accordance with the manufacturer's instructions. The PathHunter signals were measured using an EnVision plate reader (PerkinElmer Inc.). The responses to 0.3% DMSO and 1 μM OX-A were used to represent the 0% and 100% responses, respectively.

2.7.5. Evaluations of phosphorylation of ERK1/2 and CREB

Intracellular phosphorylation of ERK1/2 on Thr202/Tyr204 and CREB on Ser133 were detected using an HTRF phospho-ERK assay kit (Cat.# 64AERPEG, Cisbio Bioassays) and HTRF phospho-CREB assay kit (Cat.# 63ADK052PEG, Cisbio Bioassays), respectively, in accordance with the manufacturer's instructions with minor modifications. hOX2R/CHO-EA cells were stimulated with TAK-925 for 30 min at 37 °C in assay buffer (HBSS with 20 mM HEPES, pH 7.4, and 0.1% BSA) in the ERK1/2 assay or for 45 min at 37 °C in assay buffer in the CREB assay. Cells were lysed during a 1-h incubation with the lysis buffer at room temperature. Anti-phospho-ERK1/2 d2 antibody and anti-phospho-ERK1/2 cryptate antibody or anti-phospho-CREB d2 antibody and anti-phospho-CREB cryptate antibody diluted in detection buffer were then added to the cells. After a 2-h incubation at room temperature in the ERK1/2 assay or after overnight incubation at room temperature in the CREB assay, HTRF signals were detected using an EnVision plate reader (PerkinElmer Inc.). The responses to 0.3% DMSO and 3 μM OX-A were deemed to be the 0% and 100% responses, respectively.

2.7.6. OX2R selectivity assay

Activity of compound against various enzymes, receptors, and ion channels (106 targets in total) was evaluated at Eurofins Panlabs Discovery Services (Taipei, Taiwan).

2.7.7. Slice electrophysiology study

Experiments were performed on slices of the posterior hypothalamus containing the tuberomammillary nucleus (TMN) from 3- to 4-week-old male WT mice (C57BL/6J mice). The animals were quickly decapitated and each brain was placed in an ice-cold cutting solution (252 mM sucrose, 26 mM $NaHCO_3$, 10 mM glucose, 6 mM $MgCl_2$, 2.5 mM KCl, 0.5 mM $CaCl_2$, and 1.25 mM NaH_2PO_4) saturated with carbogen (95% O_2/5% CO_2). Slices were cut at a thickness of 300 μm with a microslicer (VT1200S, Leica Microsystems, Wetzlar, Germany) and transferred to ACSF made up of (in mM): 124 NaCl, 5 KCl, 1.2 NaH_2PO_4, 1.5 $MgCl_2$, 2.5 $CaCl_2$, 10 glucose, 24 $NaHCO_3$, and perfused with ACSF at a flow rate of 1–2 mL/min in the recording chamber at least 1 h before starting the recording. Current clamp recordings were carried out at 32–33 °C using a borosilicate pipette filled with intracellular solution (135 mM K-gluconate, 10 mM NaCl, 10 mM HEPES, 0.2 mM EGTA, 4 mM MgATP, 0.3 mM Na_2GTP, adjusted to pH 7.3 with KOH). Pharmacological effects on the change of firing rate were performed in the absence of tetrodotoxin (TTX) and on the change of resting membrane potential in the presence of TTX (1 μM). Signals were recorded using an Axopatch 200B amplifier and a Digidata 1322A digitizer board, bandpass filtered at 2 kHz, sampled at 10 kHz (Molecular Devices, CA, USA), and analyzed with pClamp10.3 software (Molecular Devices). Histaminergic neurons recorded from the TMN (which was recognizable at the ventral surface of the posterior hypothalamus as a small and dense structure) were identified by the presence of the transient outward current and the inwardly rectifying current activated by hyperpolarization.

2.8. In vivo study

2.8.1. c-fos immunofluorescence staining and quantitative analysis in orexin/ataxin-3 mice

TAK-925 (3 mg/kg) or vehicle (0.5% methylcellulose saline) was administered SC. Mice were sacrificed 1.5 h after drug administration, and then transcardial perfusion fixation with 4% paraformaldehyde was performed. The brain was dissected and sliced into 40-μm thick sections using a cryostat (Leica Microsystems). One in six slices was used for immunofluorescence staining. The sections were incubated in blocking solution (3% BSA in PBS-0.01% Triton X-100 [PBS-TX]) for 1 h at room temperature; incubated with the anti-c-Fos (9F6) rabbit monoclonal antibody (1:1000 in blocking solution, #2250 Cell Signaling Technology) for 24 h at 4 °C; incubated with a secondary antibody (1:200 in blocking solution, Biotin-SP-conjugated AffiniPure Donkey anti-rabbit IgG (H + L) #711–065-152, Jackson Immuno Research) for 1 h at room temperature; incubated with Streptavidin Alexa Fluor 488 conjugate (1:100 in blocking solution, #S11223 Thermo Fisher Scientific Inc.) and propidium iodide (1:1000 in blocking solution, #P3566 Thermo Fisher Scientific Inc.) for 1 h at room temperature; and mounted on slides with coverslip application using PermaFluor Aqueous Mounting Medium.

For quantitative analysis, images were obtained using an INCell 2000 (GE Healthcare UK, Ltd., Little Chalfont, UK) analyzer. The preprocessing of the images and quantitative analysis were then performed. First, the brain sections containing the region of interest (ROI) were cropped from the image of the whole slide using ImageJ software. Square-shaped ROIs with the size of 150 × 150 pixels (75 × 75 pixels for the supraoptic nucleus) were drawn, and quantification was performed. The signals with area below 20 pixels and above 200 pixels were removed.

2.8.2. EEG surgical procedure and data analysis in WT and OX2R KO mice

Implantation of EEG/EMG electrodes was performed as described previously (Chemelli et al., 1999). Briefly, mice were anesthetized with pentobarbital sodium (50 mg/kg, intraperitoneal, Somnopentyl®, Kyoritsu Seiyaku, Tokyo, Japan) and fixed to a stereotaxic apparatus (Kopf Instruments, Tujunga, CA, USA). For EEG recording, two stainless steel screw electrodes (Biotex, Kyoto, Japan) were chronically implanted into the cortex (1.0 mm anterior to the bregma and 1.5 mm lateral to the midline, 1.0 mm anterior to the lambda and 1.5 mm lateral to the midline) using coordinates from the atlas of Paxinos and Franklin (Paxinos and Franklin, 2012). These electrodes were placed subcranially over the dura. For EMG recording, stainless steel wire electrodes (Biotex) were implanted bilaterally into the dorsal neck muscle. All electrodes were connected to a miniature receptacle, and the entire assembly was fixed to the skull with dental cement (GC, Tokyo, Japan). For ICV administration, mice were simultaneously implanted with a guide cannula (AG-4, Eicom, Kyoto, Japan) into the left lateral ventricle (0.3 mm posterior to the bregma, 0.9 mm lateral to the midline, 2.4 mm depth from skull surface). After at least a 1-week recovery period in home cages, the mice were used for EEG recording.

EEG/EMG recordings were performed as described previously (Chemelli et al., 1999). EEG/EMG signals were amplified, filtered (EEG, 0.5–100 Hz; EMG, 16–200 Hz), digitized at a sampling rate of 200 Hz, and recorded using VitalRecorder® (Kissei Comtec Co., Ltd., Nagano, Japan). SleepSign® (Kissei Comtec Co., Ltd.) was used to automatically classify the sleep/wakefulness states in 4-s epochs as wakefulness, non-REM (NREM) sleep, or REM sleep according to standard criteria, and to calculate the time spent in wakefulness, number of episodes, and duration of wakefulness. Each stage was characterized as follows: wakefulness, low-amplitude EEG and high-voltage EMG activities; NREM sleep, high-amplitude slow EEG, and low-voltage EMG activities; and

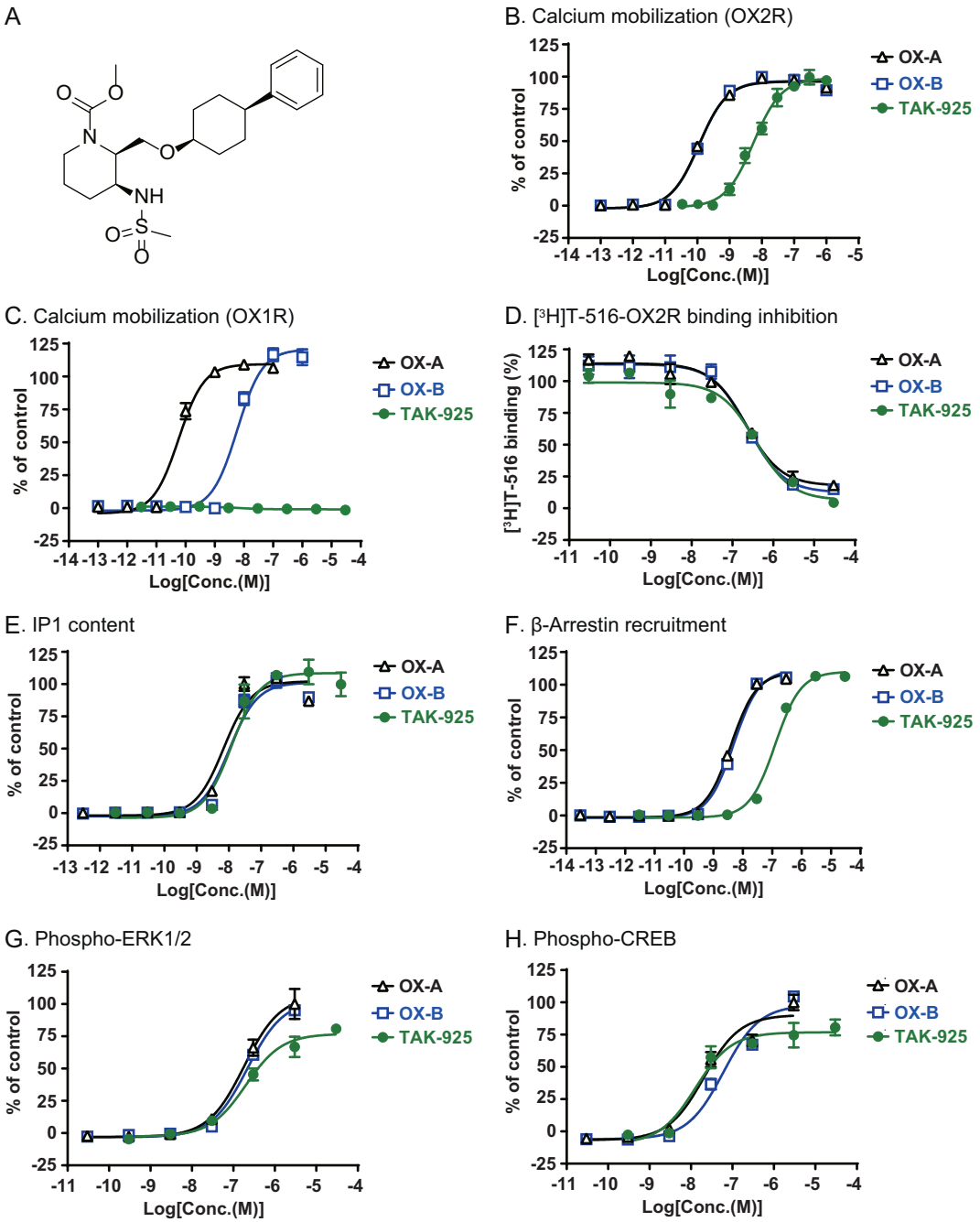

Fig. 1. TAK-925 selectively bound to OX2R and activated its downstream signals in CHO cells expressing hOX2R.
(A) Chemical structure of TAK-925.
(B) Effect of TAK-925 on calcium mobilization in hOX2R/CHO-K1 cells. The responses to 100 nM OX-A represented the 100% response. Mean ± S.D., $n = 4$.
(C) Effect of TAK-925 on calcium mobilization in hOX1R/CHO-K1 cells. The responses to 100 nM OX-A represented the 100% response. Mean ± S.D., n = 4.
(D) Binding activity of TAK-925 to OX2R assessed by inhibition of binding between a tritium-labeled OX2R agonist, [^{3}H]T-516, and Expi293F cell membranes expressing hOX2R. The responses to 100 μM unlabeled T-516 and 0.3% DMSO were used to represent the 0% and 100% responses, respectively. Mean ± S.D., n = 4.
(E) Effect of TAK-925 on intracellular accumulation of IP1 in hOX2R/CHO-EA cells. The cells were stimulated with TAK-925 for 4 h at 37 °C, and then intracellular IP1 levels were measured. The responses to 1 μM OX-A represented the 100% response. Mean ± S.D., n = 4.
(F) Effect of TAK-925 on β-arrestin recruitment in hOX2R/CHO-EA cells. The β-arrestin was assessed using the PathHunter assay kit. The responses to 1 μM OX-A represented the 100% response. Mean ± S.D., n = 4.
(G) Effect of TAK-925 on intracellular phosphorylation of ERK1/2 at Thr202/Tyr204. hOX2R/CHO-EA cells were stimulated with TAK-925 for 30 min at 37 °C, and phospho-ERK1/2 was then detected. The responses to 3 μM OX-A represented the 100% response. Mean ± S.D., n = 4.
(H) Effect of TAK-925 on intracellular phosphorylation of CREB on Ser133. hOX2R/CHO-EA cells were stimulated with TAK-925 for 45 min at 37 °C, and phospho-CREB was then detected. The responses to 3 μM OX-A represented the 100% response. Mean ± S.D., n = 4.

REM sleep, theta-dominated EEG/EMG atonia. EEG spectral analysis was performed by fast Fourier transform using SleepSign. EEG frequency band (0–80 Hz) was divided into five frequency bands: delta (0.75–4 Hz), theta (6–10 Hz), alpha (10–13 Hz), beta (13–30 Hz), and gamma (30–80 Hz). EEG power density was expressed as a percentage of the mean total EEG power for each sleep/wakefulness state.

2.9. Statistics

All *in vitro* data except the electrophysiology study data were analyzed using XLfit (IDBS, MA, USA), and 50% effective concentration (EC_{50}) values or IC_{50} values was calculated by logistic regression analysis from the data expressed as % of control. These data are expressed as the mean ± standard deviation (S.D.) in this report. In the electrophysiology study and c-fos quantitative analysis, the pairwise differences between groups were identified using Student's *t*-test. In the EEG/EMG study, the significant differences were analyzed by Williams' test or Shirley-Williams' test for multiple doses of [Ala^{11}, D-Leu^{15}]-OX-B and TAK-925. The pairwise differences between groups were identified using a paired *t*-test. These data are expressed as the mean ± standard error of the mean (S.E.M.) in this report. Values of $P \leq .05$ were considered significant.

3. Results

3.1. TAK-925 selectively bound to OX2R and activated OX2R-downstream signals in CHO cells expressing hOX2R

First, we characterized OX2R-agonistic activities of TAK-925 (Fig. 1A) in hOX2R/CHO-K1 cells using orexin peptides as positive controls. OX-A, OX-B, and TAK-925 dose-dependently increased calcium mobilization in hOX2R/CHO-K1 cells with an EC_{50} of 0.11 nM, 0.11 nM, and 5.5 nM, respectively (Fig. 1B). TAK-925 up to 30 μM did not induce calcium mobilization in hOX1R/CHO-K1 cells under the conditions that allowed OX-A and OX-B to induce calcium mobilization with an EC_{50} of 0.058 nM and 5.9 nM, respectively (Fig. 1C). Therefore, TAK-925 had > 5000-fold OX2R selectivity over OX1R. TAK-925 was an orthosteric, full agonist for OX2R with no positive allosteric modulation activity; TAK-925 did not affect the EC_{50} value of OX-A in a calcium mobilization assay using hOX2R/CHO-K1 cells (Fig. S1, Table S1).

To explore the binding affinity/site of TAK-925 on OX2R, we next established a binding assay with membrane fractions of hOX2R-transfected Expi293F cells and an OX2R-selective radioligand [^{3}H]T-516 (Fig. S2A). T-516 had a > 6000-fold OX2R selectivity against OX1R in calcium mobilization assays (EC_{50}: 4.3 nM for OX2R and > 30,000 nM for OX1R) (Fig. S2B). [^{3}H]T-516 bound to the membrane fractions of hOX2R-transfected Expi293F cells with a single saturable high-affinity binding site (Kd = 48 nM) (Fig. S2C). In this assay, OX-A, OX-B, and TAK-925 inhibited the binding of [^{3}H]T-516 to the membrane fraction with an IC_{50} of 230 nM, 250 nM, and 390 nM, respectively (Fig. 1D). These data suggest that TAK-925 and orexin peptides share the same binding site on OX2R.

Several studies have reported that OX2R signaling may be mediated by multiple G-proteins (not only by Gq, but also Gs and Gi proteins) and other proteins such as β-arrestin (Sakurai et al., 1998; Zhu et al., 2003; Dalrymple et al., 2011). Activation of Gq protein-coupled receptor leads to the generation of inositol 1,4,5-trisphosphate (IP3) through activation of phospholipase C. IP3 is quickly degraded into IP1 in cells; thus, we examined the effects of TAK-925 on IP1 production in hOX2R/CHO-EA cells using orexin peptides as controls. OX-A, OX-B, and TAK-925 increased IP1 contents with an EC_{50} of 5.0 nM, 10 nM, and 15 nM, respectively, in hOX2R/CHO-EA cells (Fig. 1E). We next evaluated β-arrestin recruitment in hOX2R/CHO-EA cells (Dalrymple et al., 2011). OX-A, OX-B, and TAK-925 increased β-arrestin recruitment with an EC_{50} of 3.5 nM, 4.1 nM, and 110 nM, respectively, in hOX2R/CHO-EA cells (Fig. 1F). OX2R activation by orexin peptides induced ERK1/2 phosphorylation and CREB phosphorylation *via* protein kinase C signaling in OX2R-expressed CHO cells (Guo and Feng, 2012). We also examined the effects of TAK-925 on ERK1/2 signals and CREB signals by quantifying phosphorylation of ERK1/2 and CREB in hOX2R/CHO-EA cells. Similar to orexin peptides, TAK-925 induced phosphorylation of ERK1/2 (EC_{50} values of OX-A, OX-B, and TAK-925 were 190 nM, 210 nM, and 240 nM, respectively) and CREB (EC_{50} values of OX-A, OX-B, and TAK-925 were 25 nM, 150 nM, and 20 nM, respectively) (Fig. 1G and H).

The OX2R selectivity of TAK-925 was further characterized by measuring its inhibitory or stimulatory activities against enzymes and receptors. > 50% inhibition or stimulation by 10 μM of TAK-925 was considered to be a significant response. TAK-925 did not induce a significant response in 106 target molecules (Tables S2 and S3).

3.2. TAK-925 activated physiological OX2R in the mouse TMN in vitro

We examined the effects of TAK-925 on physiological OX2R using whole-cell patch-clamp techniques. Histaminergic neurons in the TMN receive projections of orexin neurons located in the hypothalamus (Marcus et al., 2001). These histaminergic neurons express high levels of OX2R, but not OX1R (Sakurai, 2007; Mieda et al., 2011); thus, activation of OX2R can be assessed by measuring the membrane potential and neuron firing of these cells. [Ala^{11}, D-Leu^{15}]-OX-B, an OX-B analog with higher OX2R selectivity (230-fold selectivity against OX1R, Fig. S3) compared to OX-B (54-fold selectivity against OX1R, Fig. 1B and C), was used as a control. As previously reported (Irukayama-Tomobe et al., 2017), histaminergic neurons in the TMN showed no spontaneous firing under our recording conditions (Fig. 2A). [Ala^{11}, D-Leu^{15}]-OX-B at 300 nM depolarized membrane potential and significantly increased firing rate ($P \leq .05$, Fig. 2A). TAK-925 at 300 nM also induced a depolarization of membrane potential and significantly increased the spontaneous firing rate of histaminergic neurons in the TMN ($P \leq .05$, Fig. 2B). This effect of TAK-925 was abolished by pretreatment with 10 μM of an OX2R antagonist, compound 1 m (Fig. 2C). The whole cell patch clamp recording in the presence of 1 μM tetrodotoxin to block basal firing revealed that both [Ala^{11}, D-Leu^{15}]-OX-B and TAK-925 induced depolarization of histaminergic neurons in the TMN with an EC_{50} of 154 nM and 22 nM, respectively (Fig. 2D and E).

3.3. Peripheral administration of TAK-925 activated physiological OX2R in the mouse TMN in vivo

We next administered TAK-925 SC to orexin/ataxin-3 mice, and then characterized neuronal activation in various brain regions, including TMN, using c-fos as a marker. TAK-925 (3 mg/kg) was administered to orexin/ataxin-3 mice at zeitgeber time (ZT) 5. At 1.5 h after administration of TAK-925, mice were sacrificed, and their brains were used for c-fos immunostaining. TAK-925 significantly increased the number of c-fos-positive cells (green) in the TMN (Fig. 3A) and other brain regions except suprachiasmatic nucleus (SCH), locus ceruleus (LC), and pedunculopontine nucleus (PPN) ($P \leq .05$, Fig. 3A and B).

3.4. TAK-925 increased wakefulness in WT mice, but not in OX2R KO mice, during their sleep phase

Activation of the orexin system by ICV of OX-A promotes wakefulness in rodents (Mieda et al., 2004). In this study, we used [Ala^{11}, D-Leu^{15}]-OX-B as a positive control. [Ala^{11}, D-Leu^{15}]-OX-B was administered to WT mice (C57BL/6J mice) (0.3 and 3 nmol, ICV at ZT5, Fig. 4A), and then EEG/EMG were recorded for 1 h. [Ala^{11}, D-Leu^{15}]-OX-B significantly increased wakefulness ($P \leq .01$ at 0.3 and 3 nmol, Figs. 4B and S4A), accompanied by a decrease in NREM sleep ($P \leq .01$ at 0.3 and 3 nmol, Fig. S4B) and REM sleep (Fig. S4C) in WT mice. We

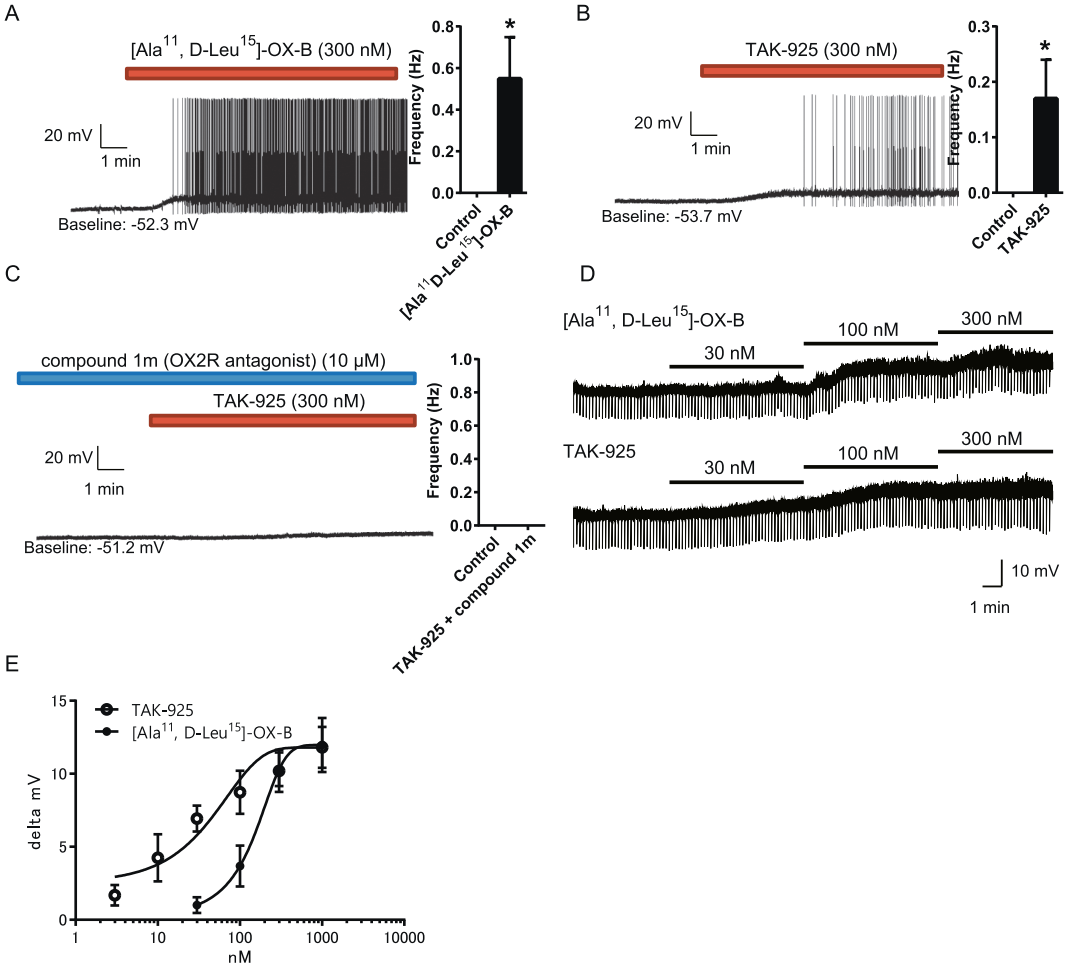

Fig. 2. TAK-925 activated physiological OX2R in the mouse TMN *in vitro*.
(A and B) Effect of [Ala[11], D-Leu[15]]-OX-B or TAK-925 on membrane potential and neuron firing by electrophysiological study with slices containing TMN isolated from 3- to 4-week-old WT mice (C57BL/6J mice). Representative data and accumulation data showing the effect of 300 nM [Ala[11], D-Leu[15]]-OX-B (n = 10) (A) or TAK-925 (n = 8) (B). Mean ± S.E.M. Pairwise difference between the control group and OX-B-treated group was identified using Student's t-test. *$P \leq .05$.
(C) Effect of TAK-925 on membrane potential and neuron firing in the presence of 10 μM compound 1 m, an OX2R antagonist, investigated by electrophysiological study with slices containing the TMNs isolated from 3- to 4-week-old WT mice. Mean ± S.E.M., n = 9. There was no significant difference between the control group and the co-treatment (TAK-925 + compound 1 m) group by Student's t-test.
(D and E) Dose-dependent increase in membrane potential by TAK-925 in the presence of 1 μM tetrodotoxin to block neuron firing. (D) Representative data showing the effect of [Ala[11], D-Leu[15]]-OX-B and TAK-925. A rectangular hyperpolarizing current pulses (−20 pA, 500 ms, 0.16 Hz) were applied to monitor changes in the input resistance of the neuron. (E) Dose-response curves of TAK-925 and [Ala[11], D-Leu[15]]-OX-B. Recordings from 4 to 5 mice for each data point. TAK-925 (3, 10, 1000 nM): n = 4, TAK-925 (100, 300 nM): n = 5, TAK-925 (30 nM) and [Ala[11], D-Leu[15]]-OX-B (30, 100, 300, 1000 nM): n = 6. TMN, tuberomammillary nucleus.

next evaluated the effects of TAK-925 on sleep/wake status in mice during their sleep phase. After administrations of TAK-925 (SC) at ZT5, EEG/EMG was recorded for 1 h (Fig. 4A). TAK-925 significantly increased wakefulness in WT mice ($P \leq .05$ at 1 mg/kg and $P \leq .001$ at 3 mg/kg, Figs. 4C and S4D), but not in OX2R KO mice at up to 10 mg/kg (Fig. 4D). Concomitantly, TAK-925 (SC) significantly decreased NREM sleep ($P \leq .05$ at 1 mg/kg and $P \leq .001$ at 3 mg/kg, Fig. 4E) and REM sleep ($P \leq .001$ at 3 mg/kg, Fig. 4F) in WT mice. EEG spectral analysis showed that TAK-925 had little or no effect on EEG power density during wakefulness, NREM sleep, and REM sleep in WT mice during their sleep phase (Figs. S5A and S5B).

4. Discussion

Patients with narcolepsy suffer from distressing symptoms such as EDS and cataplexy. Currently available medications for NT1, including psychostimulants (eg, modafinil and methylphenidate), antidepressants (clomipramine and venlafaxine), and sedatives (sodium oxybate) have limited efficacy and adverse effects (Inoue et al., 2013; Thorpy, 2015; Barateau et al., 2016). Modafinil is often used as first-line therapy for EDS in NT1; however, it has limited efficacy: mean sleep latencies determined by the maintenance of wakefulness test were prolonged by 2.8 min in the modafinil-treated group compared to the placebo group (Inoue et al., 2013), and modafinil did not improve cataplexy (Thorpy, 2015; Barateau et al., 2016). Antidepressants such as clomipramine can be used for cataplexy treatment; they do not, however, improve EDS (Thorpy, 2015). Hence, medications are generally used in combination to treat EDS and cataplexy. In clinical practice, these medications may have adverse effects, such as headache, nausea, insomnia, and neuropsychiatric symptoms (eg, anxiety, irritability and aggressiveness) (Thorpy, 2015; Barateau et al., 2016). Thus, there is a large unmet need for more effective and safer therapies to better address the multiple symptoms of narcolepsy.

Loss of orexin-producing neurons in the lateral hypothalamus is associated with narcolepsy (Nishino et al., 2000; Peyron et al., 2000; Thannickal et al., 2000). It is important to note that OX2R KO mice exhibited both a fragmentation of sleep/wake states and cataplexy-like episodes, while OX1R KO mice had no overt behavioral abnormalities

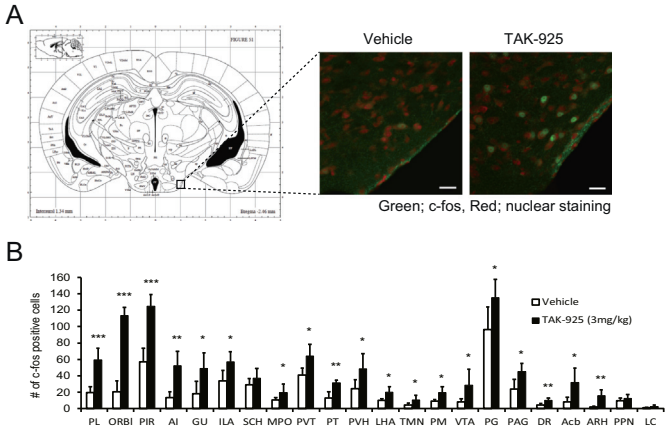

Fig. 3. TAK-925 increased neural activity in various brain regions in orexin/ataxin-3 mice.

(A) Effect of TAK-925 on neuronal activity in the TMN detected by c-fos induction as a neuronal activity marker in orexin/ataxin-3 mice. Immunohistochemistry was performed with anti-c-fos antibody to detect c-fos in sections of brain, including the TMN, recovered from orexin/ataxin-3 mice at 1.5 h after administration of TAK-925 (3 mg/kg). Representative results. White bar = 20 μm. c-fos staining (green), nuclear staining (red). The illustration on the left was cited from the Mouse Brain Atlas.(Paxinos and Franklin, 2012) (B) The number of c-fos-positive cells in various regions of brain in mice. PL, prelimbic area; ORBl, orbital area; PIR, piriform cortex; AI, angranulargranular insular area; GU, granular insular cortex; ILA, infralimbic; SCH, suprachiasmatic nucleus; MPO, medial preoptic area; PVT, paraventricular nucleus of thalamus; PT, parataenial nucleus; PVH, paraventricular nucleus of hypothalamus; LHA, lateral hypothalamic area; TMN, tuberomammillary nucleus; PM, premammillary nucleus; VTA, ventral tegmental area; PG, pontine gray; PAG, periaqueductal gray; DR, dorsal nucleus raphe; Acb, accumbens nucleus; ARH, arcuate nucleus; PPN, pedunculopontine nucleus; LC, locus ceruleus. These areas were referenced from the Mouse Brain Atlas.(Paxinos and Franklin, 2012) n = 5, Mean ± S.E.M. Pairwise difference between vehicle- and TAK-925-treated groups (3 mg/kg. s.c.) was identified using Student's *t*-test. $^{*}P \leq .05$, $^{**}P \leq .01$, $^{***}P \leq .001$. (For interpretation of the references to color in this figure legend, the reader is referred to the web version of this article.)

and exhibited only mild fragmentation of sleep/wake cycles (Tsujino and Sakurai, 2009). Thus, OX2R appears to play a pivotal role in the pathophysiology of narcolepsy. Compared with OX2R KO mice, OX1R/2R double KO mice showed stronger narcolepsy-like phenotypes: greater sleep/wake fragmentation, a larger number of direct transitions from wakefulness to REM sleep, and cataplexy-like episodes (Willie et al., 2003; Tsujino and Sakurai, 2009). Therefore, OX1R may also contribute to the pathogenesis of narcolepsy-like symptoms in mice (Tsujino and Sakurai, 2009). One may consider that activation of both OX1R and OX2R may be needed to fully address symptoms in NT1. However, by fully activating OX2R, narcolepsy symptoms can theoretically be alleviated to the levels of OX1R KO mice with no obvious abnormality. Since activation of OX1R in the ventral tegmental area may increase the risks of addictive behaviors *via* activation of the dopaminergic reward system (Nakamura et al., 2000; Xu et al., 2013), OX2R-selective agonists may be preferred over OX1R/OX2R dual agonists as a novel therapy for NT1 (Willie et al., 2003). As narcolepsy-like symptoms in orexin/ataxin-3 mice were ameliorated by ICV administration of orexin peptides, orexin receptors and their downstream neural pathways remained functionally intact even after lengthy orexin deficiency in mice (Mieda et al., 2004). In patients with NT1, there is no reduction of OX2R mRNA, although there are no data regarding OX2R protein levels or the function of its downstream neural pathways (Mishima et al., 2008). Overall, replacement therapy with OX2R-selective agonists is considered to be a promising therapeutic option for NT1, although careful assessment of the function of OX2R and its downstream pathways are necessary.

Orexin peptides are not suitable for clinical use as a drug, due to their lack of BBB penetration (Fujiki et al., 2003). Thus, discovery of OX2R activators with better physiochemical properties is critically important. There are several types of GPCR activators, such as orthosteric or allosteric agonists with full or partial activation, and positive allosteric modulators. Some biased agonists are reported to have different signal transduction and pharmacological profiles from those of orthosteric agonists (Violin et al., 2014; Pupo et al., 2016). It is unknown which downstream signals are involved in OX2R-mediated physiological actions of orexin peptides. Thus, clinical characterization of the OX2R activators with a signal transduction pattern similar to that of orexin peptides was a key to understanding the therapeutic potential of OX2R-selective activation for NT1.

In our study, we discovered TAK-925 and carefully characterized its *in vitro* and *in vivo* profile. TAK-925 showed potent agonistic activity for OX2R (EC_{50} value of 5.5 nM) with > 5000-fold selectivity against OX1R (Fig. 1B and C); TAK-925 showed no positive allosteric modulation activity for OX2R (Fig. S1 and Table S1). TAK-925 did not induce a significant response to 106 other target molecules even at 10 μM (Tables S2 and S3), suggesting that TAK-925 is a highly potent and selective OX2R agonist *in vitro*. Similar to OX-A and OX-B, TAK-925 inhibited selective binding of [^{3}H]T-516 to OX2R (Fig. 1D); thus, TAK-925 and orexin peptides may share a binding site on OX2R. The activation pattern of OX2R downstream signals, such as IP1 production, β-arrestin recruitment, phospho-ERK increase, and phospho-CREB increase, by TAK-925 was similar to those induced by orexin peptides *in vitro* (Fig. 1E–H). Furthermore, *in vitro* electrophysiological analysis revealed that TAK-925 selectively activates physiological OX2R and promotes neuronal activities of histaminergic neurons in the mouse TMN, which were blocked by an OX2R-specific antagonist (Fig. 2). Moreover, TAK-925 (SC) robustly increased c-fos positive cells in TMN and other brain regions in orexin/ataxin-3 mice which had low levels of endogenous orexin peptides, demonstrating that peripherally administered TAK-925 can enter the brain and activate OX2R on the neurons (Fig. 3). TAK-925 may also indirectly induce c-fos positive cells in these brain regions by modulating neural circuits. For example, stimulation of OX2R on histaminergic neuron in TMN may activate multiple monoaminergic circuits through increase in histamine release (Flink et al., 2015; Scammell et al., 2019). Importantly, TAK-925 promoted wakefulness (Fig. 4C) and decreased both NREM and REM sleep in WT mice (Fig. 4E and F), but not in OX2R KO mice (Fig. 4D), during their sleep phase. Therefore, TAK-925 would induce wakefulness *via* OX2R activation in mice. Further studies would be needed to understand OX2R down-stream pathway to induce arousal. The modulation pattern of wakefulness and NREM and REM sleep duration by TAK-925 was similar to that produced by [Ala^{11}, D-Leu^{15}]-OX-B. Wake-promoting effects of TAK-925 in WT mice were observed for < 1 h after administration (Fig. S4D). This is due to the short half-life of TAK-925 in mice. Drug administration approaches for proof-of-concept studies in human would be designed with careful consideration of pharmacokinetic profile of TAK-925 in human.

5. Conclusions

In conclusion, TAK-925 is a novel, small-molecule OX2R-selective agonist with the potential to selectively modulate OX2R and its downstream signals similar to those produced by orexin peptides. TAK-925 induced neural activation and arousal after peripheral administration. TAK-925 may provide a unique opportunity to investigate the therapeutic potential of OX2R selective activation for NT1 and other hypersomnia disorders. TAK-925 is under investigation in clinical development as an orexin replacement therapy and a potential new treatment option for patients with hypersomnia (Clincaltrials.gov Registry Identifier: NCT03332784).

Supplementary data to this article can be found online at https://doi.org/10.1016/j.pbb.2019.172794.

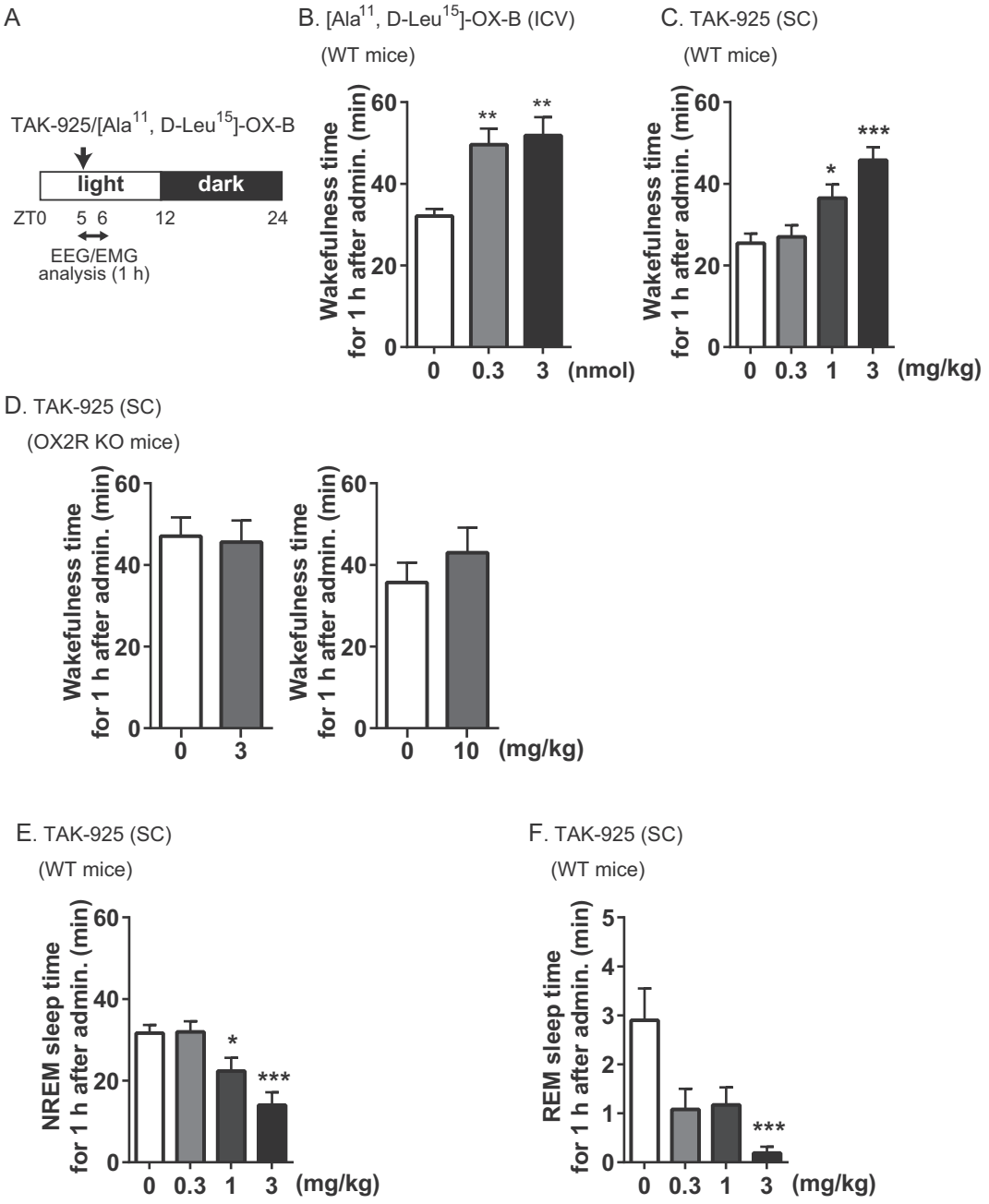

Fig. 4. TAK-925 increased wakefulness in WT mice, but not in OX2R KO mice, during their sleep phase.
(A) Experimental procedure for measurement of EEG/EMG. [Ala^{11}, D-Leu^{15}]-OX-B (ICV) or TAK-925 (SC) was administered to mice at ZT5, and then EEG/EMG were recorded for 1 h. ZT, zeitgeber time.
(B) Effect of [Ala^{11}, D-Leu^{15}]-OX-B (0.3 and 3 nmol, ICV) on wakefulness in WT mice (C57BL/6J mice) during their sleep phase. Mean ± S.E.M., n = 6. $^{**}P \leq .01$, compared with the vehicle-treated mice (Williams' test).
(C) Effect of TAK-925 (0.3, 1, and 3 mg/kg, SC) on wakefulness in WT mice during their sleep phase. Mean ± S.E.M., $n = 8$. $^{*}P \leq .05$, $^{***}P \leq .001$, compared with the vehicle-treated mice (Williams' test).
(D) Effect of TAK-925 (3 and 10 mg/kg, SC) on wakefulness in OX2R KO mice during their sleep phase. Mean ± S.E.M., n = 6. No significant difference by paired *t*-test.
(E) Effect of TAK-925 (0.3, 1, and 3 mg/kg, SC) on NREM sleep in WT mice during their sleep phase. Mean ± S.E.M., n = 8. $^{*}P \leq .05$, $^{***}P \leq .001$, compared with the vehicle-treated mice (Williams' test).
(F) Effect of TAK-925 (0.3, 1, and 3 mg/kg, SC) on REM sleep in WT mice during their sleep phase. Mean ± S.E.M., n = 8. $^{***}P \leq .001$, compared with the vehicle-treated mice (Shirley-Williams' test).

Funding disclosure

This work was funded by Takeda Pharmaceutical Company Limited. All authors are/were employee of Takeda Pharmaceutical Company Limited.

Acknowledgements

We wish to express our sincere thanks to Dr. Takeshi Sakurai for his advice and for introducing experimental mice. We also thank Ayumi Kawano, Sayuri Nakamura, and Eiji Sunahara, for their support.

References

Barateau, L., Lopez, R., Dauvilliers, Y., 2016. Management of narcolepsy. Curr. Treat. Options Neurol. 18 (10), 43. https://doi.org/10.1007/s11940-016-0429-y.

Chemelli, R.M., Willie, J.T., Sinton, C.M., Elmquist, J.K., Scammell, T., Lee, C., Richardson, J.A., Williams, S.C., Xiong, Y., Kisanuki, Y., Fitch, T.E., Nakazato, M., Hammer, R.E., Saper, C.B., Yanagisawa, M., 1999. Narcolepsy in orexin knockout mice: molecular genetics of sleep regulation. Cell 98 (4), 437–451. https://doi.org/10.1016/s0092-8674(00)81973-x.

Dalrymple, M.B., Jaeger, W.C., Eidne, K.A., Pfleger, K.D., 2011. Temporal profiling of orexin receptor-arrestin-ubiquitin complexes reveals differences between receptor subtypes. J. Biol. Chem. 286 (19), 16726–16733. https://doi.org/10.1074/jbc.M111.223537.

Flink, G., Folgering, J., Cremers, T., Westerink, B., Dremencov, E., 2015. Interaction between brain histamine and serotonin, norepinephrine, and dopamine system: in vivo microdialysis and electrophysiology study. J. Mol. Neurosci. 56 (2), 320–328. http://doi https://doi.org/10.1007/s12031-015-0536-3.

Fujiki, N., Yoshida, Y., Ripley, B., Mignot, E., Nishino, S., 2003. Effects of IV and ICV hypocretin-1 (orexin A) in hypocretin receptor-2 gene mutated narcoleptic dogs and IV hypocretin-1 replacement therapy in a hypocretin-ligand-deficient narcoleptic dog. Sleep 26 (8), 953–959. https://doi.org/10.1093/sleep/26.8.953.

Fujimoto, T., Kunitomo, J., Tomata, Y., Nishiyama, K., Nakashima, M., Hirozane, M., Yoshikubo, S., Hirai, K., Marui, S., 2011. Discovery of potent, selective, orally active benzoxazepine-based Orexin-2 receptor antagonists. Bioorg. Med. Chem. Lett. 21 (21), 6414–6416. https://doi.org/10.1016/j.bmcl.2011.08.093.

Golden, E.C., Lipford, M.C., 2018. Narcolepsy: diagnosis and management. Cleve. Clin. J. Med. 85 (12), 959–969. https://doi.org/10.3949/ccjm.85a.17086.

Guo, Y., Feng, P., 2012. OX2R activation induces PKC-mediated ERK and CREB phosphorylation. Exp. Cell Res. 318 (16), 2004–2013. https://doi.org/10.1016/j.yexcr.2012.04.015.

Hara, J., Beuckmann, C.T., Nambu, T., Willie, J.T., Chemelli, R.M., Sinton, C.M., Sugiyama, F., Yagami, K., Goto, K., Yanagisawa, M., Sakurai, T., 2001. Genetic ablation of orexin neurons in mice results in narcolepsy, hypophagia, and obesity. Neuron 30 (2), 345–354. https://doi.org/10.1016/s0896-6273(01)00293-8.

Inoue, Y., Takasaki, Y., Yamashiro, Y., 2013. Efficacy and safety of adjunctive modafinil treatment on residual excessive daytime sleepiness among nasal continuous positive airway pressure-treated japanese patients with obstructive sleep apnea syndrome: a double-blind placebo-controlled study. J. Clin. Sleep Med. 9 (8), 751–757. https://doi.org/10.5664/jcsm.2912.

Irukayama-Tomobe, Y., Ogawa, Y., Tominaga, H., Ishikawa, Y., Hosokawa, N., Ambai, S., Kawabe, Y., Uchida, S., Nakajima, R., Saitoh, T., Kanda, T., Vogt, K., Sakurai, T., Nagase, H., Yanagisawa, M., 2017. Nonpeptide orexin type-2 receptor agonist ameliorates narcolepsy-cataplexy symptoms in mouse models. Proc. Natl. Acad. Sci. U. S. A. 114 (22), 5731–5736. https://doi.org/10.1073/pnas.1700499114.

Jacobson, L.H., Chen, S., Mir, S., Hoyer, D., 2017. Orexin OX2 receptor antagonists as sleep aids. Curr Top Behav Neurosci 33, 105–136. https://doi.org/10.1007/7854_2016_47.

de Lecea, L., Kilduff, T.S., Peyron, C., Gao, X., Foye, P.E., Danielson, P.E., Fukuhara, C., Battenberg, E.L., Gautvik, V.T., Bartlett 2nd, F.S., Frankel, W.N., van den Pol, A.N., Bloom, F.E., Gautvik, K.M., Sutcliffe, J.G., 1998. The hypocretins: hypothalamus-specific peptides with neuroexcitatory activity. Proc. Natl. Acad. Sci. U. S. A. 95 (1), 322–327. https://doi.org/10.1073/pnas.95.1.322.

Lin, L., Faraco, J., Li, R., Kadotani, H., Rogers, W., Lin, X., Qiu, X., de Jong, P.J., Nishino, S., Mignot, E., 1999. The sleep disorder canine narcolepsy is caused by a mutation in the hypocretin (orexin) receptor 2 gene. Cell 98 (3), 365–376. https://doi.org/10.1016/s0092-8674(00)81965-0.

Marcus, J.N., Aschkenasi, C.J., Lee, C.E., Chemelli, R.M., Saper, C.B., Yanagisawa, M., Elmquist, J.K., 2001. Differential expression of orexin receptors 1 and 2 in the rat brain. J. Comp. Neurol. 435 (1), 6–25. https://doi.org/10.1002/cne.1190.

Mieda, M., Willie, J.T., Hara, J., Sinton, C.M., Sakurai, T., Yanagisawa, M., 2004. Orexin peptides prevent cataplexy and improve wakefulness in an orexin neuron-ablated model of narcolepsy in mice. Proc. Natl. Acad. Sci. U. S. A. 101 (13), 4649–4654. https://doi.org/10.1073/pnas.0400590101.

Mieda, M., Hasegawa, E., Kisanuki, Y.Y., Sinton, C.M., Yanagisawa, M., Sakurai, T., 2011. Differential roles of orexin receptor-1 and -2 in the regulation of non-REM and REM sleep. J. Neurosci. 31 (17), 6518–6526. https://doi.org/10.1523/JNEUROSCI.6506-10.2011.

Mishima, K., Fujiki, N., Yoshida, Y., Sakurai, T., Honda, M., Mignot, E., Nishino, S., 2008. Hypocretin receptor expression in canine and murine narcolepsy models and in hypocretin-ligand deficient human narcolepsy. Sleep 31 (8), 1119–1126. https://www.ncbi.nlm.nih.gov/pmc/articles/PMC2542958/.

Nagahara, T., Saitoh, T., Kutsumura, N., Irukayama-Tomobe, Y., Ogawa, Y., Kuroda, D., Gouda, H., Kumagai, H., Fujii, H., Yanagisawa, M., Nagase, H., 2015. Design and synthesis of non-peptide, selective Orexin receptor 2 agonists. J. Med. Chem. 58 (20), 7931–7937. https://doi.org/10.1021/acs.jmedchem.5b00988.

Nakamura, T., Uramura, K., Nambu, T., Yada, T., Goto, K., Yanagisawa, M., Sakurai, T., 2000. Orexin-induced hyperlocomotion and stereotypy are mediated by the dopaminergic system. Brain Res. 873 (1), 181–187. https://doi.org/10.1016/s0006-8993(00)02555-5.

Nishino, S., Kanbayashi, T., 2005. Symptomatic narcolepsy, cataplexy and hypersomnia, and their implications in the hypothalamic hypocretin/orexin system. Sleep Med. Rev. 9 (4), 269–310. https://doi.org/10.1016/j.smrv.2005.03.004.

Nishino, S., Ripley, B., Overeem, S., Lammers, G.J., Mignot, E., 2000. Hypocretin (orexin) deficiency in human narcolepsy. Lancet 355 (9197), 39–40. https://doi.org/10.1016/S0140-6736(99)05582-8.

Paxinos, G., Franklin, K.B.J., 2012. The Mouse Brain in Stereotaxic Coordinates, Fourth edition. Academic Press, London, UK.

Peyron, C., Faraco, J., Rogers, W., Ripley, B., Overeem, S., Charnay, Y., Nevsimalova, S., Aldrich, M., Reynolds, D., Albin, R., Li, R., Hungs, M., Pedrazzoli, M., Padigaru, M., Kucherlapati, M., Fan, J., Maki, R., Lammers, G.J., Bouras, C., Kucherlapati, R., Nishino, S., Mignot, E., 2000. A mutation in a case of early onset narcolepsy and a generalized absence of hypocretin peptides in human narcoleptic brains. Nat. Med. 6 (9), 991–997. https://doi.org/10.1038/79690.

Pupo, A.S., Duarte, D.A., Lima, V., Teixeira, L.B., Parreiras, E.S.L.T., Costa-Neto, C.M., 2016. Recent updates on GPCR biased agonism. Pharmacol. Res. 112, 49–57. https://doi.org/10.1016/j.phrs.2016.01.031.

Sakurai, T., 2007. The neural circuit of orexin (hypocretin): maintaining sleep and wakefulness. Nat. Rev. Neurosci. 8 (3), 171–181. https://doi.org/10.1038/nrn2092.

Sakurai, T., Amemiya, A., Ishii, M., Matsuzaki, I., Chemelli, R.M., Tanaka, H., Williams, S.C., Richardson, J.A., Kozlowski, G.P., Wilson, S., Arch, J.R., Buckingham, R.E., Haynes, A.C., Carr, S.A., Annan, R.S., McNulty, D.E., Liu, W.S., Terrett, J.A., Elshourbagy, N.A., Bergsma, D.J., Yanagisawa, M., 1998. Orexins and orexin receptors: a family of hypothalamic neuropeptides and G protein-coupled receptors that regulate feeding behavior. Cell 92 (4), 573–585. https://doi.org/10.1016/s0092-8674(00)80949-6.

Sateia, M.J., 2014. International classification of sleep disorders-third edition: highlights and modifications. Chest 146 (5), 1387–1394. https://doi.org/10.1378/chest.14-0970.

Scammell, T., Jackson, A., Franks, N., Wisden, W., Dauvilliers, Y., 2019. Histamine: neural circuits and new medications. Sleep 42 (1), 1–8. https://doi.org/10.1093/sleep/zsy183.

Thannickal, T.C., Moore, R.Y., Nienhuis, R., Ramanathan, L., Gulyani, S., Aldrich, M., Cornford, M., Siegel, J.M., 2000. Reduced number of hypocretin neurons in human narcolepsy. Neuron 27 (3), 469–474. https://doi.org/10.1016/s0896-6273(00)00058-1.

Thorpy, M.J., 2015. Update on therapy for narcolepsy. Curr. Treat. Options Neurol. 17 (5), 347. https://doi.org/10.1007/s11940-015-0347-4.

Tsujino, N., Sakurai, T., 2009. Orexin/hypocretin: a neuropeptide at the interface of sleep, energy homeostasis, and reward system. Pharmacol. Rev. 61 (2), 162–176. https://doi.org/10.1124/pr.109.001321.

Violin, J.D., Crombie, A.L., Soergel, D.G., Lark, M.W., 2014. Biased ligands at G-protein-coupled receptors: promise and progress. Trends Pharmacol. Sci. 35 (7), 308–316. https://doi.org/10.1016/j.tips.2014.04.007.

Willie, J.T., Chemelli, R.M., Sinton, C.M., Tokita, S., Williams, S.C., Kisanuki, Y.Y., Marcus, J.N., Lee, C., Elmquist, J.K., Kohlmeier, K.A., Leonard, C.S., Richardson, J.A., Hammer, R.E., Yanagisawa, M., 2003. Distinct narcolepsy syndromes in Orexin receptor-2 and Orexin null mice: molecular genetic dissection of non-REM and REM sleep regulatory processes. Neuron 38 (5), 715–730. https://doi.org/10.1016/s0896-6273(03)00330-1.

Xu, T.R., Yang, Y., Ward, R., Gao, L., Liu, Y., 2013. Orexin receptors: multi-functional therapeutic targets for sleeping disorders, eating disorders, drug addiction, cancers and other physiological disorders. Cell. Signal. 25 (12), 2413–2423. https://doi.org/10.1016/j.cellsig.2013.07.025.

Zhu, Y., Miwa, Y., Yamanaka, A., Yada, T., Shibahara, M., Abe, Y., Sakurai, T., Goto, K., 2003. Orexin receptor type-1 couples exclusively to pertussis toxin-insensitive G-proteins, while orexin receptor type-2 couples to both pertussis toxin-sensitive and -insensitive G-proteins. J. Pharmacol. Sci. 92 (3), 259–266.